Ultramicroscopy 29 (1989) 183–191
North-Holland, Amsterdam

DYNAMICAL THEORY OF SPOT SPLITTING IN RHEED

L.D. MARKS and Y. MA

Materials Research Center, Northwestern University, Evanston, Illinois 60208, USA

Received at Editorial Office October–November 1988; presented at Conference May 1988

The dynamical diffraction explanation of spot splitting in reflection electron microscopy (REM) and reflection high energy electron diffraction (RHEED) is described within a Bloch wave formalism. The positions of the spots match exactly those measured experimentally and described previously using kinematical theory. Numerically calculated results for misoriented GaAs (001) and Pt(111) surfaces are presented.

1. Introduction

The important role of surface steps in areas such as chemisorption [1,2] and crystal growth by techniques such as molecular beam epitaxy (MBE) [3] is well known. One of the earliest and still most common methods of exploring surface steps is via their effects upon diffraction patterns in either low energy electron diffraction (LEED) or in RHEED. A particularly simple case is when the steps form a regular periodic structure, essentially a vicinal surface, see for instance fig. 1. The presence of an additional surface periodicity due to this step array leads to extra diffraction spots, most readily observable as a splitting of the single spot from a perfect surface into a number of satellites, as well documented in both LEED [4–6] and RHEED [7] experiments. Pukite et al. [8,9] demonstrated that the spacing of these satellite spots could be well described using simple kinematical theory, whilst Hsu and Cowley [10] have demonstrated in imaging REM experiments that the spot splitting was consistent with the presence of a periodic array of surface steps. However, while kinematical theory can very often correctly predict the presence and position of diffraction features, as a rule it is totally unreliable as far as the intensities are concerned, at least for electron diffraction.

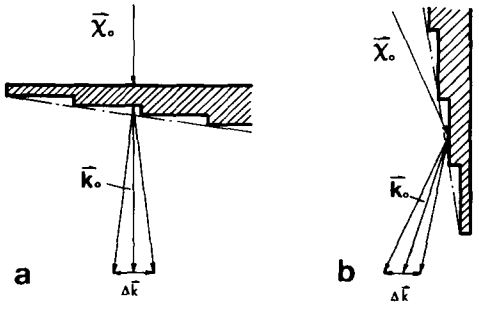

Fig. 1. Comparison of the experimental configurations that lead to spot splitting in (a) transmission high-energy electron diffraction (THEED) and (b) RHEED, In (a) is shown the typical geometry for transmission through a wedge-shaped crystal, in (b) reflection from a vicinal surface.

The intent of this paper is to present a more rigorous dynamical diffraction explanation of step spot splitting. As we will show, the spot splitting is the reflection equivalent of what are often called refractive multiplets in transmission diffraction. In addition, we present calculated results for the intensities of the satellite spots for a number of simple surfaces.

2. Physics of spot splitting

In order to understand the source of the spot splitting, it is important to draw the analogies between transmission diffraction from a wedged-shaped crystal and reflection diffraction from an

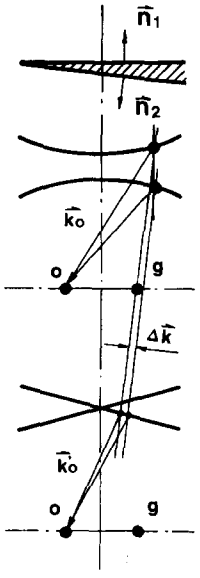

Fig. 2. Illustration of Bloch wave matching using the dispersion surface for a wedge-shaped crystal in THEED. Matching between the vacuum level dispersion (equal energy) surfaces which are shown at the bottom to two crystal dispersion surface, shown at the top along n_1 at the entrance surface and n_2 at the exit surface leads to a pair of outgoing spots. (With a more detailed analysis there is one satellite spot for each Bloch wave within the crystal.) It should be noted that the spot splitting depends upon both the wedge angle and the dispersion surface structure, and as a rule a kinematical model gives incorrect results.

array of steps. The basic point is that a stepped surface (assuming monatomic steps) can be considered as a bulk crystal cut at an angle to a "flat" low-index plane, whilst a wedge crystal can be considered as a specimen cut on at least one surface at an angle to such a plane, see for instance fig. 1. (We are ignoring surface relaxations around steps, a point which we will return to later in the discussion.) Within a Bloch wave formalism, which is equally valid in the transmission [11] and reflection geometries [12], we consider that inside the crystal Bloch waves are excited which have to be matched across the entrance/exit surfaces of the crystal. In transmission the wave is matched at both the top (entrance) and the bottom (exit) surfaces, with reflection ignored in general; see fig. 2. In reflection diffraction the reflected waves are taken into account when matching at the top surface, which is both the entrance and exit surface as illustrated in fig. 3.

To match correctly the incoming wave above the crystal and the Bloch waves within, one has to, geometrically, draw lines normal to the crystal surfaces from the incoming wave to the dispersion surface, and then lines again normal to the exit surface out to Ewald spheres for the diffracted beams as illustrated in figs. 2 and 3. (Details of the standard dispersion surface analysis can be found in numerous texts and articles, for instance ref. [11].) In transmission two sets of lines are drawn for the top and bottom surfaces respectively, leading to spot splitting as experimentally and theoretically discussed by a number of authors [13,14]. In reflection the entrance surface is also the exit surface, and spot splitting occurs if the surface is at an angle to a low-index flat surface or zone axis, by a directly analogous process. (Creating a surface cut at a small angle to a flat surface is almost identical to a vicinal surface with an array of surface steps and no surface relaxations; we will return to this point in the discussion.) The relationship between the spot splitting and the misorientation of the surface can be more readily seen by reference to fig. 3. From such a diagram the positions of the spots can be indexed by the relationship

$$\phi_{\pm g} = \sin^{-1}\left[\cos\left(\theta_i + \beta^{\text{eff}}\right) \mp \frac{g}{k}\sin\beta^{\text{eff}}\right], \tag{1}$$

$$\alpha_{0\pm g} = \sin^{-1}\left[\cos\left(\theta_i + \beta^{\text{eff}}\right) \mp \frac{g}{k}\sin\beta^{\text{eff}}\right] - \left(\tfrac{1}{2}\pi - \theta_i - \beta^{\text{eff}}\right), \tag{2}$$

where

$$\beta^{\text{eff}} = \tan^{-1}(\tan\beta\cos\Phi), \tag{3}$$

with $\phi_{\pm g}$ the angle between the reflected electron beam and the surface normal, $\alpha_{0\pm g}$ the angle between the specularly reflected beam and the reflected beam g, β the misorientation angle, Φ the azimuthal angle; and g refers to the particular Ewald sphere onto which the matching occurs. We have adopted the notation of indexing the satellite spots via the particular Ewald sphere that they arise from with a subscript "s" to denote satellite, and we are using the specularly reflected beam as

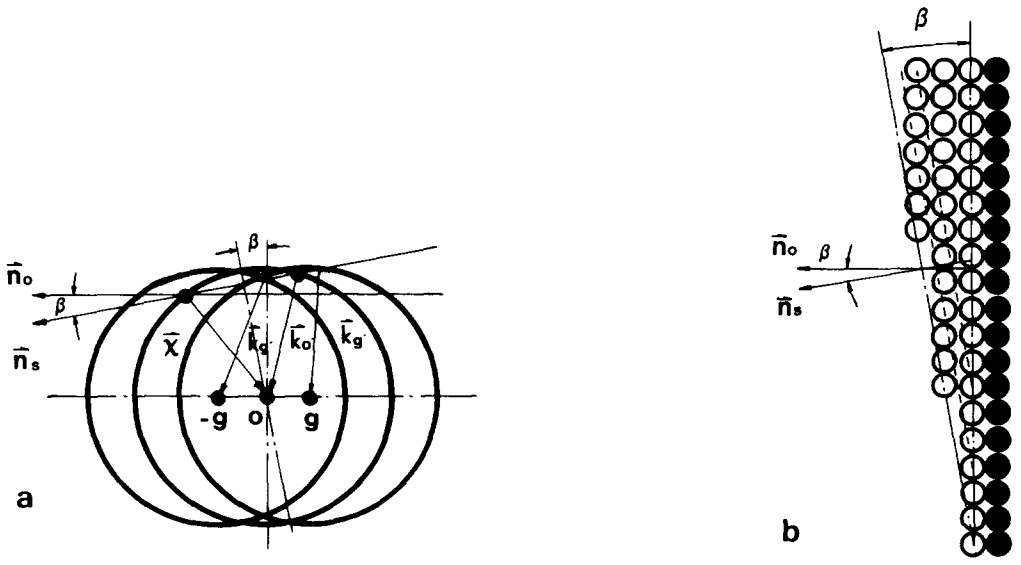

Fig. 3. Illustration of Bloch wave matching for RHEED in (a), with the relative geometry of the beams with respect to the surface shown in (b). Matching along n_s, the surface normal, leads to satellite spots around each outgoing wave; for instance the spots $\pm g$ in the figure will appear as satellites around the specular beam. The satellite spots are indexed in terms of the vacuum dispersions surfaces from which they originate; for instance the satellite g in the figure is indexed as $(g)_s$ with subscripting to denote that these are satellite spots.

the natural origin since, except at an exact Bragg condition, it does not correspond to any reciprocal lattice vector translation of the incident beam and its seems illogical to employ irrational indices for diffraction spots. Here β^{eff} is the effective surface misorientation angle after taking the beam azimuth with respect to the Laue zone axis into account. This equation gives the same results as that derived using kinematical theory by Pukite et al. [8,9] if we define the specular beam as our origin; here we have derived it using dynamical theory. Using eq. (2) we can reproduce exactly the polar plot shown in fig. 2 of ref. [9] for the angular separation between the $(\bar{2}00)_s$ and $(200)_s$ spots versus the incidence azimuth angle for a fixed incident angle of $\theta_i = 65$ mrad. Although it might seem obvious that the dynamical and kinematical theories should lead to the same spot positions, in fact this is not true; for transmission diffraction through a wedge crystal the spot positions are, in fact, different since they reflect the dispersion surface structure rather than simply the wedge angle alone as predicted by kinematical theory. It should be noted that in the dispersion surface analysis the additional spots are not a consequence of the additional surface potential due to the steps, as might be thought, but are instead due to the boundary conditions.

Two points should be clarified here, the first of which is the specular beam position. One can straightforwardly show, using simple kinematical arguments, that the specular beam is reflected from the vicinal surface, not the low-index surface; this point is not clear in the analysis of Pukite et al. [8,9]. The difference between the two is, in fact, very small as a rule, but to obtain exact agreement with the experimental data it is important to take this into account. The second point concerns the validity of eq. (1) and fig. 3a if evanescent waves are excited in the crystal. The actual internal Bloch wave states excited, whether they are evansecent or travelling, do not enter into the momentum conservation law which allows us to draw fig. 3a; for a perfect crystal without inelastic scattering there is no mechanism for momentum transfer normal to the surface (ignoring HOLZ

lines), and the only role that the Bloch wave states in the crystal have is in determining the relative amplitudes of the diffracted waves.

The above explanation of the source of the spot splitting does not, of course, specify the intensities; for this we require a dynamical calculation which we turn to in the next section.

3. Numerical results

Numerical results were calculated using a Bloch wave diagonalization method which has been described in detail elsewhere [12,15]. The presence of a vicinal surface was included in the calculations by using a surface cut at an angle to the zone axis of the crystal. (It should be noted that this ignores any effects due to surface relaxations around steps and only includes single atomic steps.) The results of the Bloch wave diagonalization calculations were transferred to standard imaging programs written at Northwestern operating on Apollo workstations, and these programs were used to produce both real space images and diffraction patterns via interfacing to a suite of image analysis routines; the details of these routines are not relevant to the results presented herein.

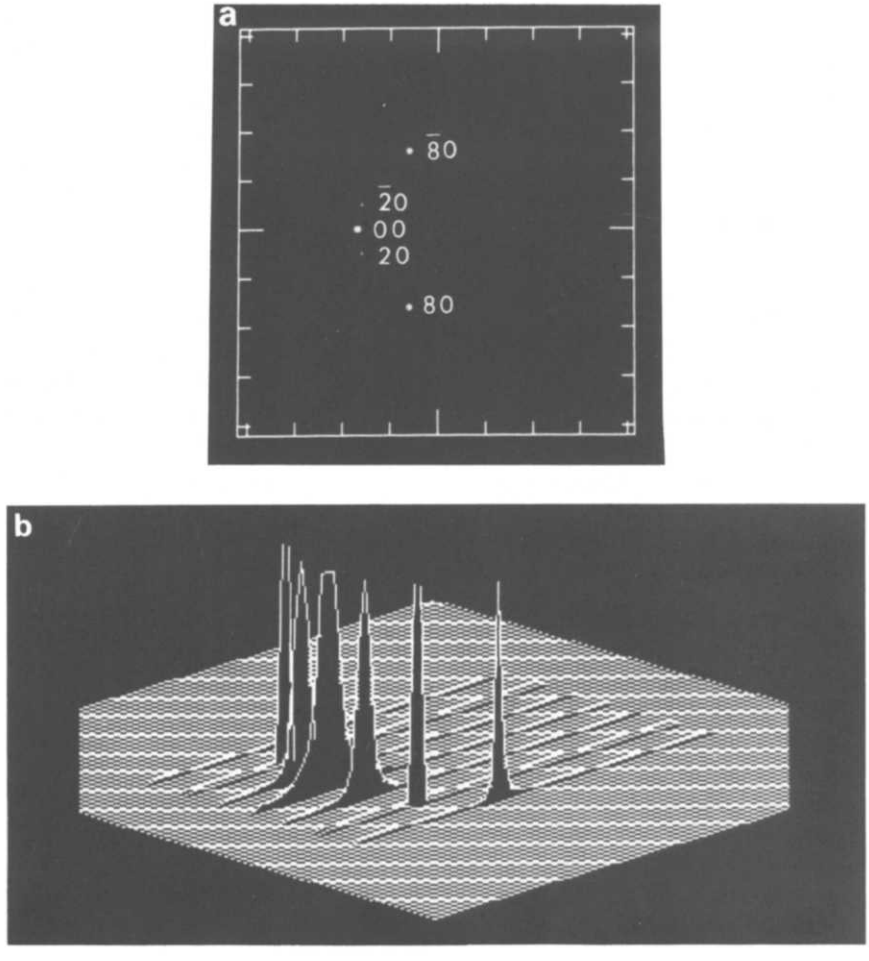

Fig. 4. Simulated RHEED patterns for a GaAs (001) surface with the incident beam near to [010] and a glancing angle of 2.4° without any absorption: (a) diffraction pattern and (b) y-modulation representation of the same. In (a) some of the stronger satellite spots are indexed.

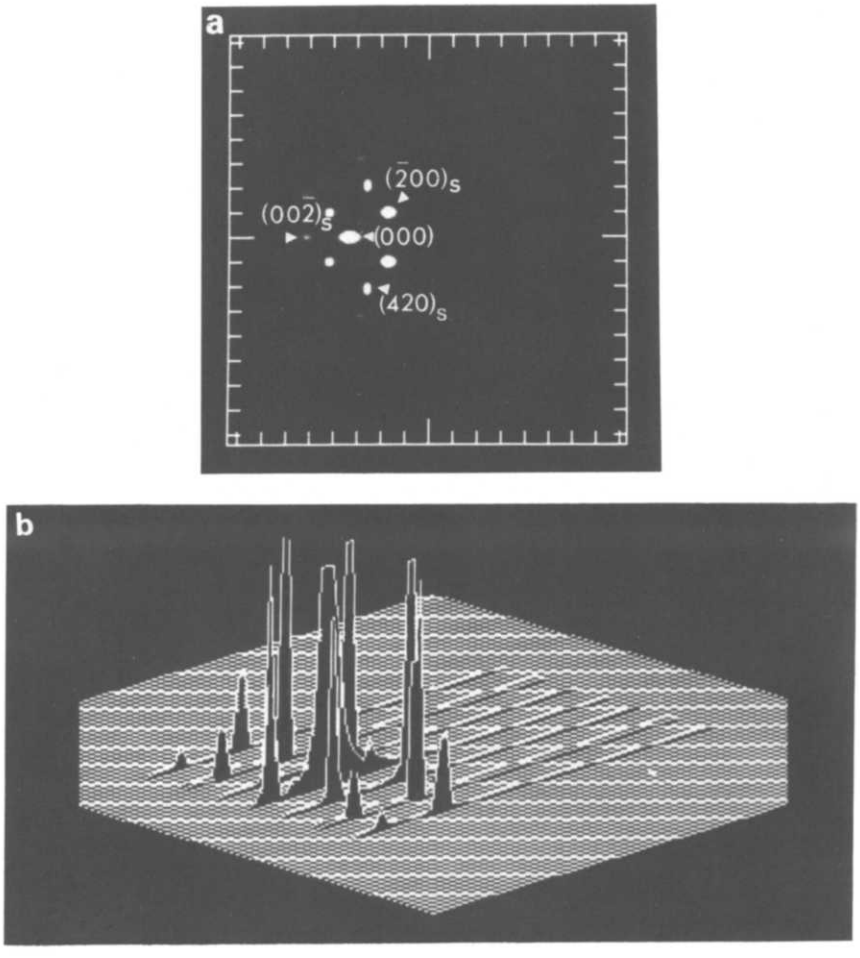

Fig. 5. Simulated RHEED patterns for a GaAs (001) surface for the same conditions as in fig. 4 but with a vicinal surface 2.5° off (010) zone axis: (a) diffraction pattern and (b) y-modulation representation of the same. In (a) some of the stronger satellite spots are indexed.

As an example of the effect of an inclined surface, fig. 4a shows a simulated RHEED pattern from a perfect GaAs (001) surface for 100 keV electrons with the beam azimuth along [010] and a glancing angle of 2.4° without any absorption. In the calculation only the zero-Laue-zone Fourier coefficients of the potential have been included, so that only a single semicircular pattern from the zero-order Laue zone occurs. Fig. 4b shows a y-modulated presentation of the same data as in fig. 4a which shows just single peaks. (In these and all the subsequent y-modulation graphs the finite width of the diffracted beams is due to the numerical representation, and the scale is saturated so that the weaker peaks can be more readily seen.) In this and all subsequent y-modulation graphs the well separated peaks correspond to the satellite spots. For comparison, fig. 5 shows the results for the same relative orientation, but now a vicinal surface 2.5° off (010) zone axis. Spot splitting occurs because of the surface misorientation, and the spots are also slightly streaked normal to the surface. The pattern changes from a semicircle to an intensity distribution in two dimensions. (It should be noted that the intensities of some of the satellite spots are so low that they are not ap-

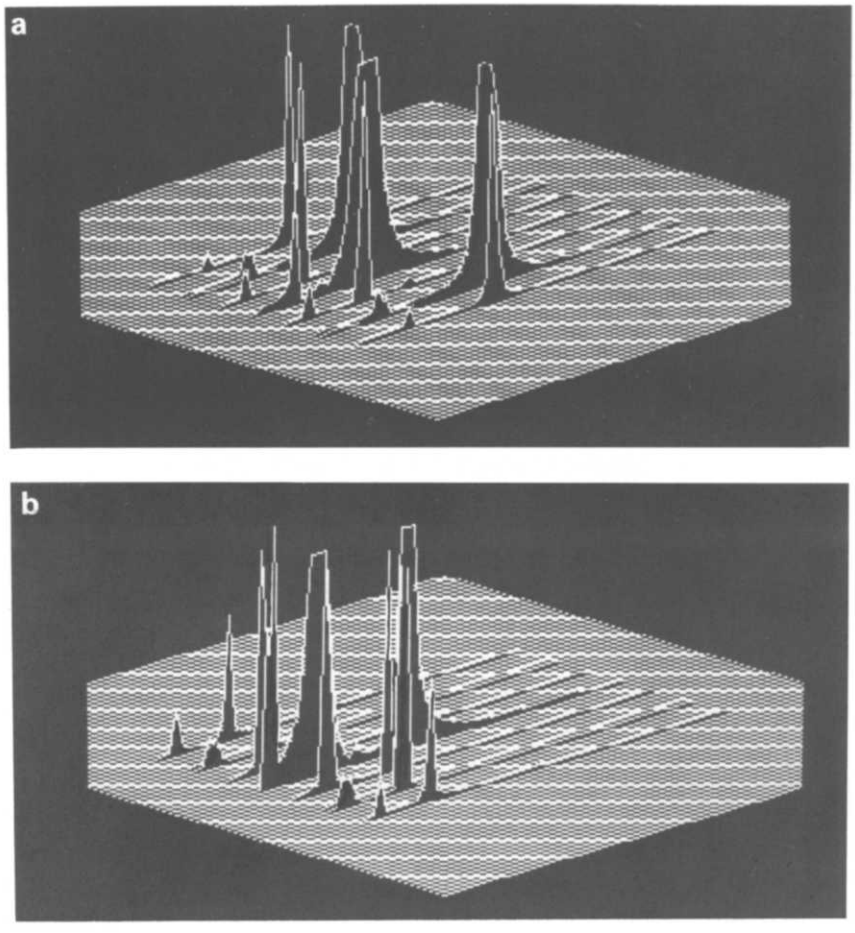

Fig. 6. y-Modulated simulated RHEED patterns for the same conditions as for fig. 4 except for incident angles of 27 and 50 mrad in (a) and (b), respectively.

parent in the figures.) The pattern also shows that each reciprocal rod has two strong spots, which is consistent with experimental data [7–10].

Eq. (2) also indicates that the spacing between the spots increases as the incident angle is reduced. This is demonstrated in fig. 6 which shows y-modulated images for the same conditions as fig. 4, except that in fig. 6a it is 27 mrad, and in fig. 6b 50 mrad. The variation in the spot splitting is quite obvious.

The separation of the spots decreases with the surface misorientation angle, until for a flat surface the spots overlap [13]. The beam azimuth changes the effective misorientation angle, i.e. the farther off the zone axis, the smaller the effective misorientation angle, as observed experimentally [7–9]. To demonstrate this point, figs. 7a and 7b show y-modulated images for the same diffraction conditions as figs. 6a and 6b, respectively, but with an azimuthal angle of 1°. The spacing between the spots in figs. 7a and 7b is obviously smaller than in figs. 6a and 6b.

The results above for GaAs show the general trend of the results. However, it may be hard to match these experimentally because we are ignoring phenomena such as surface relaxations. We have therefore calculated results for a simpler surface which is known to have little to no surface relaxation, a Pt (111) surface close to a [211] zone. Fig. 8 shows the ratio of the specularly reflected

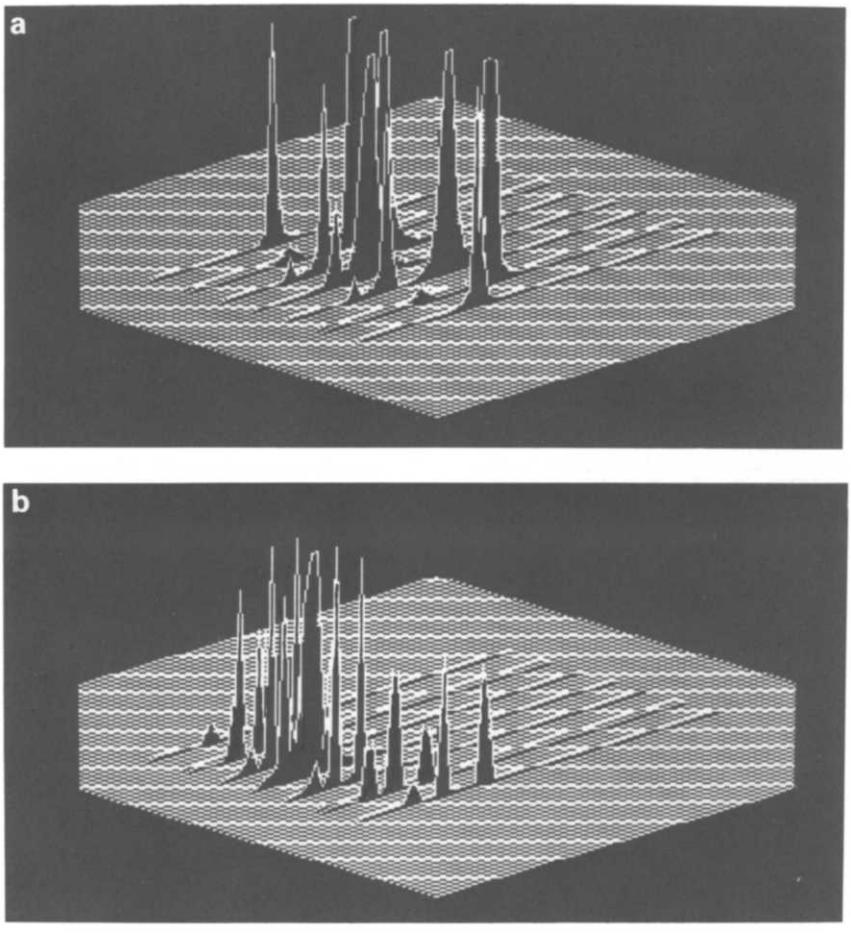

Fig. 7. y-Modulated simulated RHEED patterns for the same conditions as in figs. 6a and 6b, respectively, with a change of the azimuthal angle to 1°.

beam to the $(333)_s$ beam as a function of different azimuthal for a fixed surface misorientation angle, no absorption and 10% absorption. The $(333)_s$ beam here is that produced by matching onto the (333) Ewald sphere, as described earlier in the text, with the origin taken as the specularly reflected beam (see eqs. (1)–(3) for the position of the spots). The Pt(111) surface is believed to have very small to no surface reconstruction and is therefore a good test case. There are two obvious features in fig. 8a: (1) the intensity ratio for the case with no absorption is generally lower than that with 10% absorption, which means that absorption reduces both the total diffraction intensity and the relative satellite spot intensities; (2) the intensity ratio is lowest at the zero azimuthal angle both with and without absorption. The variations in the intensity ratio about zero azimuthal angle is possibly related to surface resonance, although this merits further exploration. Fig. 9 shows a graph of the same ratio as the function of the incidence beam angle for zero azimuthal angle with a fixed misorientation angle and no absorption. The curve shows that the intensity ratio

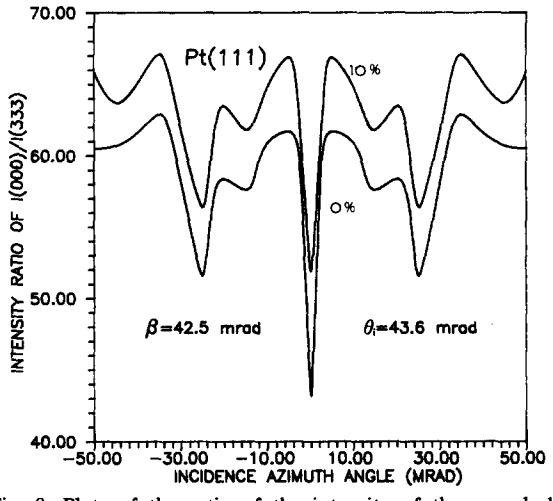

Fig. 8. Plots of the ratio of the intensity of the specularly reflected beam to the $(333)_s$ beam as a function of azimuthal angle for a fixed azimuthal angle, above with 10% absorption and below without absorption.

increases sharply when the incidence angle is close to zero, which means that the satellite spots can barely be observed at small angles. (All the calculations are for 100 kV electrons.)

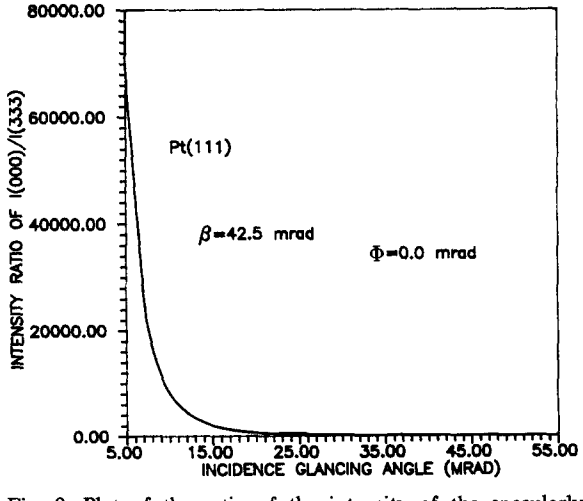

Fig. 9. Plot of the ratio of the intensity of the specularly reflected beam to the $(333)_s$ beam as described in the text for a fixed azimuthal angle as a function of the incident glancing angle.

4. Discussion and conclusion

The results that we have obtained are very encouraging in terms of understanding spot-splitting effects; for instance, we have found that in general there are two strong spots, which is qualitatively in agreement with experimental results [7–10]. At the same time we should acknowledge that some phenomena are not included in our calculations. First, we have only discussed regularly distributed surface steps, and there will quite often be irregularly distributed steps on any given surface. The effect of irregularly distributed surface steps on the diffraction pattern is hard to analyze exactly theoretically, but to first order should be equivalent to an incoherent sum of different stepped surfaces, summed over the probability of finding in any given micro-region a given step separation. This will lead to streaks in the diffraction patterns normal to the surface. Secondly, we have not included any effects due to surface relaxations or strain fields around steps; in principle there can be a relaxation of the surface stress around a step which can lead to atomic displacements, which we can consider as a strain field. The presence of such a strain field will alter the diffraction to a small but significant extent. In addition, there will also be an effect due to difference between the potential cut that we have used herein and a potential which is allowed to slowly decay into the vacuum. However, it should be noted that some preliminary calculations [16] indicate that this has only a minor effect on the diffraction pattern intensities. This is understandable since high-energy electron diffraction is only really sensitive to the core potential, not the weak interatomic potential which is what is being changed by the precise form of the surface potential. Finally, we have not here considered images of steps as obtained in REM images. In principle these can be calculated from the Bloch wave approach, but we suspect that the long-range strain field around a surface step will contribute substantially to the image contrast; this will be discussed elsewhere. In general, we think that this theoretical development gives a clear dynamical method of understanding spot splitting and related phenomena in the RHEED, although its

application to real experimental surfaces remains to be tested.

Acknowledgement

This work was supported by the National Science Foundation through the Northwestern University Materials Research Center on Grant No. DMR 85-20280.

References

[1] G.A. Somorjai, Chemistry in Two Dimensions: Surfaces (Cornell University Press, Ithaca, NY, 1981) p. 125.
[2] G.A. Somorjai, Advan. Catalysis 26 (1977) 1.
[3] K. Ploog, J. Crystal Growth 79 (1986) 887.
[4] W.P. Ellis and R.L. Schwoebel, Surface Sci. 11 (1968) 82.
[5] M. Henzler, Surface Sci. 19 (1970) 159.
[6] B.Z. Olshanetsky, S.M. Repinsky and A.A. Shklyaev, Surface Sci. 69 (1977) 205.
[7] V.S. Kikuchi and S. Nakagawa, Sci. Rept. Inst. Phys. Chem. Res. Tokyo 21 (1933) 256.
[8] P.R. Pukite and P.I. Cohen, Appl. Phys. Letters 50 (1987) 1739.
[9] P.R. Pukite, J.M. Van Hove and P.I. Cohen, Appl. Phys. Letters 44 (1983) 456.
[10] T. Hsu and J.M. Cowley, Ultramicroscopy 11 (1983) 239.
[11] A.J.F. Metherell, in: Electron Microscopy in Materials Science, Vol. 2, Eds. U. Valdrè and E. Ruedl (Luxembourg, 1976) p. 401.
[12] L.D. Marks and Y. Ma, Acta Cryst. A44 (1988) 392.
[13] J.M. Cowley and A.L.G. Rees, Nature 158 (1946) 550.
[14] G. Honjo, J. Phys. Soc. Japan 2 (1947) 133.
[15] Y. Ma and L.D. Marks, Acta Cryst. A45 (1989) 174.
[16] A.L. Bleloch, A. Howie, R.H. Milne and M.G. Walls, Ultramicroscopy 29 (1989) 175.